ISSN 1009 - 3095 *Journal of Zhejiang University(SCIENCE)* V.2, No.1, P.15 - 23, Jan. - Mar., 2001
http://www.chinainfo.gov.cn/periodical; http://www.zju.edu.cn;
http://lib.zju.edu.cn/English; http://www.zjupress.com

RESEARCH ON DISTURBANCE PROPERTIES OF SUSPENSIONS NEAR THE INJECTION AREA OF MOVING JET*

LIN Jian-zhong(林建忠), ZHOU Ze-xuan(周泽宣), WU Tao(吴涛), YOU Zhen-jiang(游振江)

(*Department of Mechanics, State Key Laboratory of Fluid Power Transmission and Control, Zhejiang University, Hangzhou 310027, P. R. China*)

Received May.12, 2000; revision accepted July 15, 2000

Abstract: The equation of the suspension-gas non-streamwise complex disturbance velocity ratio near the injection area of moving jet was theoretically derived by using a phase-coupled model and stability theory. Then the ratio curves were obtained by the finite difference method based on the asymptotic method and the Euler conservative difference scheme. Analysis of the curves yielded conclusions on the disturbance properties of suspensions and effects of the natures of the flow-field and the properties of the suspensions on the suspensions' ability to track the disturbed gas flow are presented in this paper.

Key words: disturbance property, suspension, spatial stability, moving jet, numerical computation
Document code: A **CLC number:** O359

INTRODUCTION

Moving jet containing suspensions including coal powder, droplets and so on widely exists in technical applications such as aircraft using fuel for power. Lin Jianzhong et al. (2000) whose study showed that the erosion of walls of a device varies with the change of the coherent structures caused by artificial disturbances, proposed that the wall erosion can be lessened by interfering purposefully with the coherent structures in the flow. Their numerical simulations revealed that the coherent structures influence the wall erosion by imposing changes on the motions of the suspensions. Obviously, the suspensions' motions such as deposition, collision and so on have important effect on the running efficiency of a device, So it is very necessary to determine the disturbance properties of suspensions near the injection area of a moving jet as they affect the motions of suspensions directly.

Chung and Troutt (1988) and Longmire and Eaton(1992) demonstrated that the flow-field' scoherent structure has influence on particles' dispersion. On the basis of their studies, Longmire and Eaton(1994) showed that particles' dispersion near the injection area is affected by the development of large-scale vortic structure. Apparently, it is possible that particles' dispersion can be controlled by means of changing the development of large-scale vortic structure which can be realized by imposing sound wave on the primary jet shear layers. Peterson and Samet (1988) studied the evolution of preferred unstable modes of round jet stimulated by sound wave under moderate Reynolds numbers and found that the phase-locked disturbance velocity map and measured phase-locked profile accorded well with the results of Orr-Sommerfeld linear stability analysis, showing that the effect of small particles' existence on a jet can be investigated by the linear stability theory. Neglecting the gas viscosity and the fluctuation of suspension velocity, Yang et al. (1990) studied the spatial stability of the gas-particle two-phase mixing layer and found that the existence of small particles enhances the flow stability. Sykes and Lyell(1994), considering the spatial stability of round jet full of particles found that particles can stabilize the flow-field. Ramkumar(1995) investigated the stability of stationary round jet laden with particles under small disturbance and obtained the effect of suspension property on small disturbances of different nature without consideration of the suspen-

* Projects supported by the State Education Commission's Trans-century Training Program Fund for Talents

sion disturbance property. Alfons and Gunter (1982) researched the stability of a round jet with external flow and found that external flow has clear and important effect on the stability of the flow-field. Based on and extending the researches above, the authors(1999) investigated the temporal disturbance property of particles lying on the interface of a moving two-phase jet and obtained some conclusions on the temporal disturbance properties of suspended solid particles: and can model well the potential core region of a jet. Consequently, the authors will focus on the analyses of spatial disturbance properties of suspensions near the injection area of moving jet and extract the corresponding conclusions.

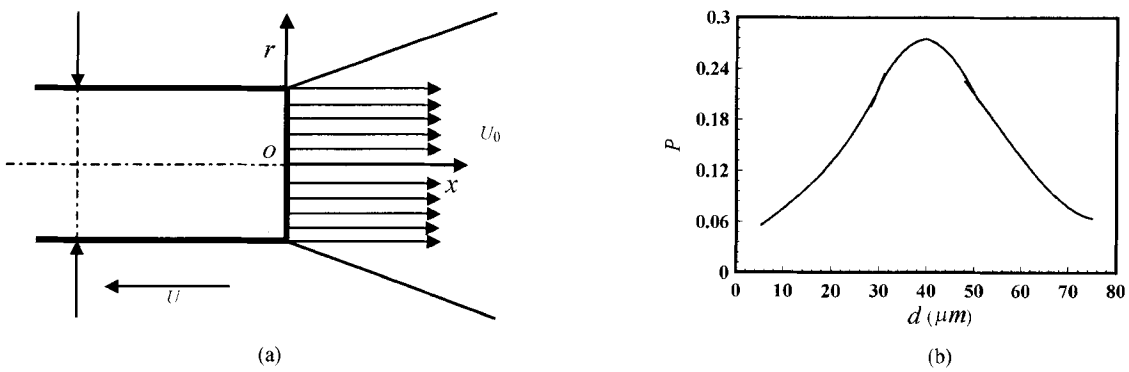

(a) (b)

Fig. 1 Moving two-phase jet
(a) jet containing suspensions; (b) suspension size distribution curve

MATHEMATICAL MODEL AND EQUATIONS

For the moving two-phase jet shown in Fig. 1, the components constituting the flow, gas and suspensions, are incompressible. It is well established that the dynamics of the large-scale structures in the near-injection area can be considered inviscid. Computations of the eigenvalues are simpler if the viscous effect is ignored. Our aim is to determine the disturbance properties of suspensions in the development of the near-injection large-scale structures. Disregarding the gas viscosity does not adversely affect our calculations. Suspensions diameters as shown in Fig. 1 are so small that we assume the modified Stokes lag is dominant. So, there exist the following equations:

$$\nabla \cdot \vec{u}_g = 0 \tag{1}$$

$$\frac{\partial \vec{u}_g}{\partial t} + \vec{u}_g \cdot \nabla \vec{u}_g = -\frac{\nabla p}{\rho_g} + \alpha_s F_g(\vec{u}_s - \vec{u}_g) \tag{2}$$

$$\frac{d\vec{u}_s}{dt} = F_s(\vec{u}_g - \vec{u}_s) \tag{3}$$

where $\vec{u}_g$ is gas velocity vector; p is pressure; ρ_g is gas density; α_s is suspension volume fraction; F_g is Stokes lag force coefficient, $\vec{F}_g = m/\rho_g$, m is Stokes lag force coefficient; u_s is suspension velocity vector; F_s is Stokes lag force coefficient, $F_s = m/\rho_s$, ρ_s , is suspension density.

In many applications of suspension-laden jets, the injector is designed to provide a tophat or nearly tophat profile. The results on the former's temporal stability was studied by the authors(1999). In most cases, the latter is real. According to Alfons and Gunter's research results(1982), the nearly tophat profile used is the profile that can model well the potential core region of the circular jet:

$$U = U_\infty + \frac{U_o - U_\infty}{2}\left\{1 - \text{th}\left[\frac{R_\theta}{4}\left(\frac{r}{R} - \frac{R}{r}\right)\right]\right\} \tag{4}$$

in which $R_\theta = 100/3\,\frac{x}{R} + 4$, x is x -coordinate, R is half of shearing thickness of moving jet; U is mean axial velocity; U_∞ is velocity of jetting device; U_o is mean x -axial velocity of the exit; r is r -coordinate; th( ) is hyperbolic tangent function.

The equations below can be used to study the response of suspensions to infinitesimal disturbance.

$$\begin{aligned} \vec{u}_j &= \vec{\bar{u}}_j + \vec{u}'_j \\ P &= \bar{p} + p' \end{aligned} \tag{5}$$

where $(\bar{\ })$ is mean variables; $()'$ is disturbance variables.

Following Ramkumar(1995), we consider $\vec{\bar{u}}_s = [\bar{u}_{sx}(r)\ 0\ 0]^T$ based on the assumption that suspensions move along the streamlines because of the neglect of the very small sediment velocity of suspensions with small diameters as shown in Fig. 1(b) compared with the characteristic velocity of the flow-field. Obviously, we can obtain further $\vec{\bar{u}}_g = \vec{\bar{u}}_s = \vec{U}$ by means of Eq. (3), $\vec{U}$ is mean velocity vector.

Considering the mean forms of Eq. (1) ~ Eq. (3), substituting the quantities in Eq. (5) into Eq. (1) ~ Eq. (3) and then linearizing the momentum equations among them, we have

$$\frac{\partial u'}{\partial x} + \frac{\partial u'_{gr}}{\partial r} + \frac{u'_{gr}}{r} + \frac{1}{r}\frac{\partial u'_{g\phi}}{\partial \phi} = 0 \tag{6}$$

$$\frac{\partial \vec{u}_g}{\partial t} + U\frac{\partial \vec{u}_g}{\partial x} + \begin{bmatrix} u'_{gr}\dfrac{dU}{dr} \\ 0 \\ 0 \end{bmatrix} = \frac{\nabla p'}{\rho_g} + \alpha_s F_g(\vec{u}_s - \vec{u}'_g) \tag{7}$$

$$\frac{\partial \vec{u}'_s}{\partial t} + U\frac{\vec{u}'_s}{\partial x} + \begin{bmatrix} u'_{sr}\dfrac{dU}{dr} \\ 0 \\ 0 \end{bmatrix} = F_s(\vec{u}_g - \vec{u}'_s) \tag{8}$$

where ϕ is ϕ – coordinate.

Based on the dynamic nature of a moving jet, it is obvious that there exist the finite disturbance condition $r = 0$ and the infinitesimal disturbance condition $r = \infty$.

Following Ramkumar (1995), the type of disturbance to be considered is

$$\begin{aligned} \vec{u}'_j &= \varepsilon R\{[U_{jx}(r)\ iU_{jr}(r)\ U_{j\phi}(r)]^T \times \exp[i(\alpha x + n\phi - \beta t)]\} \\ p' &= \rho_g \varepsilon R\{P(r)\exp[i(\alpha x + n\phi - \beta t)]\} \end{aligned} \tag{9}$$

where ε is initial value of disturbance; $[\ ]^T$ is reversion of vector; n is asymmetric order of disturbance; β is real frequency; α is complex wave number.

Substituting Eq. (9) in Eq. (6), Eq. (7) and Eq. (8), we can obtain

$$\frac{d^2P}{dr^2} + \left[\frac{1}{r} + \frac{1}{r}\frac{2\alpha}{(\beta - U\alpha)(1 + P_g)}\frac{dU}{dr}\right]\frac{dP}{dr} - \left(\alpha^2 + \frac{n^2}{r^2}\right)P = 0 \tag{10}$$

where $P_g = \dfrac{i(\beta - U\alpha)\alpha_s F_g}{(\beta - U\alpha)^2 + i2F_s(\beta - U\alpha) - F_s(F_s + \alpha_s F_g)}$.

Subsituting the disturbance pressure function in Eq. (9) in the finite disturbance condition and the infinitesimal disturbance condition, we can have

$$|P| < \infty \quad (r = 0) \tag{11}$$

$$|P| \to 0 \quad (r \to \infty) \tag{12}$$

The following suspension – gas non – streamwise complex disturbance velocity ratio equation can be obtained from Eq. (8):

$$R_a EXP(i\theta) = \frac{iF_s}{\beta - U\alpha + iF_s} \tag{13}$$

where θ is suspension – gas disturbance phase difference; R_a is amplitude of suspension – gas complex disturbance velocity ratio.

The suspension – gas streamwise complex disturbance velocity ratio equation will be discussed in another paper.

COMPUTATIONAL DATA, NUMERICAL METHOD AND RESULTS

Computational data

As an example, coal powder widely used in industry is chosen as suspension. According to the suspension shearing theory, based on the previous analyses, apparently, $m = \rho_s \sum_k^{\infty} P_k f_k / \tau_{sk}$, τ_{sk} is response time of suspension group k, $\tau_{sk} = \rho_s d_k^2 / 18\mu g$, μg is dynamic viscosity of gas, d_k is diameter of suspension group k; f_k is modified Stokes lag coefficient of suspension group k; P_k is mass percentage of suspension group k.

As for the modified coefficients f_k, we adopt the following formulation

$$f_k = 1 + 15.8341\alpha_s P_k/(1 - \alpha_s P_k)^2 - 25.4139(\alpha_s P_k)^2/(1 - \alpha_s P_k)^4 \tag{14}$$

Additionally, 68 groups of particles sampled along the industrial coal powder size distribution curve shown in Fig. 1(b) are used to evaluate the equivalent Stokes number.

Numerical method

The finite difference method is adopted to solve the eigenvalue problem posed by Eq. (10)-Eq. (12). The finite difference scheme used is the Eulerian conservative difference scheme (Kong Kang and Qin Mengzhao, 1991). Fig. 2 shows the division of the flow - field. The finite difference equation of Eq. (10) obtained with the Euler conservative difference scheme is

$$\begin{cases} P_{(n+1)} = \dfrac{1}{\Delta}\left\{d_1\left[1 + \dfrac{\Delta r}{2}f_{2(n+0.5)}\right] + \dfrac{\Delta r}{2}d_2\right\} \\ \dfrac{dP_{(n+1)}}{dr} = \dfrac{1}{\Delta}\left[d_2 - d_1\dfrac{\Delta r}{2}f_{1(n+0.5)}\right] \end{cases} \tag{15}$$

in which $f_2 = \dfrac{1}{r} + \dfrac{2\alpha}{(\beta - U\alpha)(1 + P_g)}\dfrac{dU}{dr}$,

$d_1 = P_{(n)} + \dfrac{\Delta r}{2}\dfrac{dP_{(n)}}{dr}$, $f_1 = -\left(\alpha^2 + \dfrac{n^2}{r^2}\right)$,

$d_2 = -\dfrac{\Delta r}{2}f_{1(n+0.5)}P_{(n)} + \left[1 - \dfrac{\Delta r}{2}f_{2(n+0.5)}\right]\dfrac{dP_{(n)}}{dr}$

and, $\Delta = 1 + \dfrac{\Delta r}{2}f_{2(n+0.5)} + \dfrac{(\Delta r)^2}{4}f_{1(n+0.5)}$, Δr is computational step length.

Since $\dfrac{dU}{dr}$ in Eq. (10) vanishes as $r \to 0$ and $r \to \infty$, the inner and outer solutions are given by $I_n(\alpha r)$ and $K_n(\alpha r)$ respectively (Alfons and Gunter, 1982), I_n and K_n are order of n modified Bessel functions. The matching condition at any point different from the axis and the far - field point requires that P and $\dfrac{dP}{dr}$ be continuous. Thus, P and $\dfrac{dP}{dr}$ for $r = R$ satisfy

$$\frac{dP_i(R)}{dr}/P_i(R) = \frac{dP_o(R)}{dr}/P_o(R) \tag{16}$$

where subscript i is inner part of jet and o is outer part of jet.

As we know, it is not possible that the equation above is numerically satisfying. Consequently, the matching condition must be converted to the other forms. Here, the following form is used:

$$D_{iff} = \frac{dP_i(R)}{dr}/P_i(R) - \frac{dP_o(R)}{dr}/P_o(R) \tag{17}$$

In the numerical computation, the eigenvalue α was varied until the matching condition was satisfied as to the desired accuracy. The suspension - gas non - streamwise complex disturbance velocity ratio curves were obtained after the substitution of the eigenvalue in Eq. (13).

Numerical results

The suspension-gas complex disturbance velocity ratio curve varies with the change of the suspension volume fraction in Fig. 3, 4, 5 and Fig. 6. The $\beta\theta/\Delta U$ (ΔU is jumping velocity of moving jet, characteristic velocity of the flow-field, $\Delta U = U_o - U_\infty$, θ is momentum thickness of the shearing layer of moving jet) in Fig. 3 and Fig. 4 is different from that in Fig. 5 and Fig. 6. The variations of the suspension - gas complex disturbance velocity ratio curve with the change of the suspension equivalent Stokes number ($St = 1/T_0\sum_{k=1}^{\infty} P_k f_k/\tau_{sk}$, T_0 is characteristic time, $T_0 = R/\Delta U$) are shown in Fig. 7 to Fig. 10. In addition, all the curves were obtained under the condition that $R_\theta = 10$.

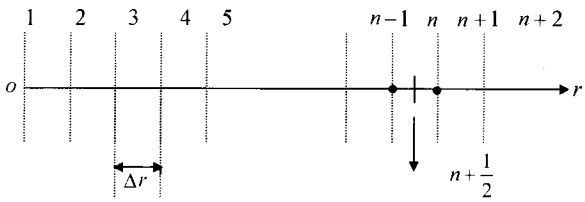

Fig. 2 Division of the flow-field

DISCUSSION AND CONCLUSIONS

1. It can be seen from Fig. 3 to Fig. 14 that whether the disturbance is symmetric or asymmetric, the amplitude of the ratio is not greater than 1. Apparently, this reveals, based on Eq. (13), that suspension disturbance velocity is less than the gas velocity. This point is in good agreement with the corresponding results with temporal disturbance obtained by the authors (1999). The agreement shows that our theoretical analyses and numerical method are reasonable.

2. We can know from Fig. 3 to Fig. 14 that whether the disturbance is symmetric or asymmetric, the suspension-gas phase difference equals zero at the critical point of the mean velocity profile, is negative between the axis and the critical point but positive between the critical point and the far-field point. These show that the suspension disturbance phase accords with the gas phase at the critical point, lags the gas phase between the axis and the critical point but leads the gas phase between the critical point and the far-field point.

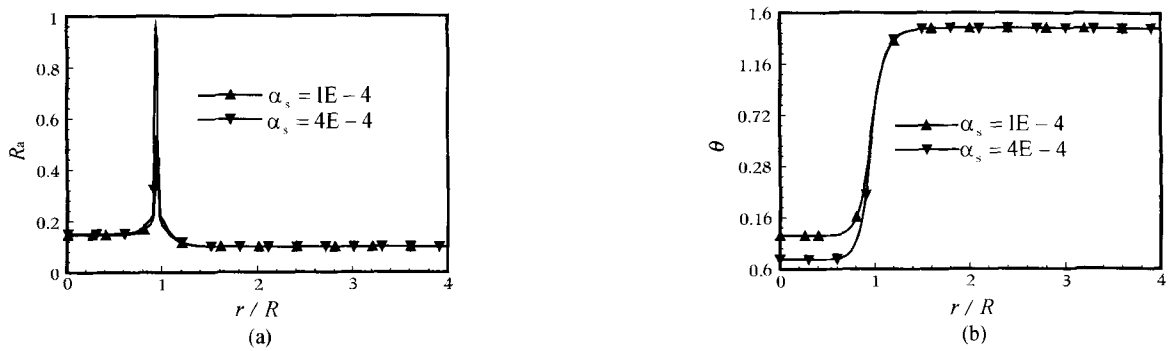

Fig. 3 Suspension-gas complex disturbance velocity ratio curves($\frac{\beta\theta}{\Delta U}$ = 0.1, U_∞ = 0, St = 10, n = 0)

(a) amplitude of velocity ratio; (b) disturbance phase difference

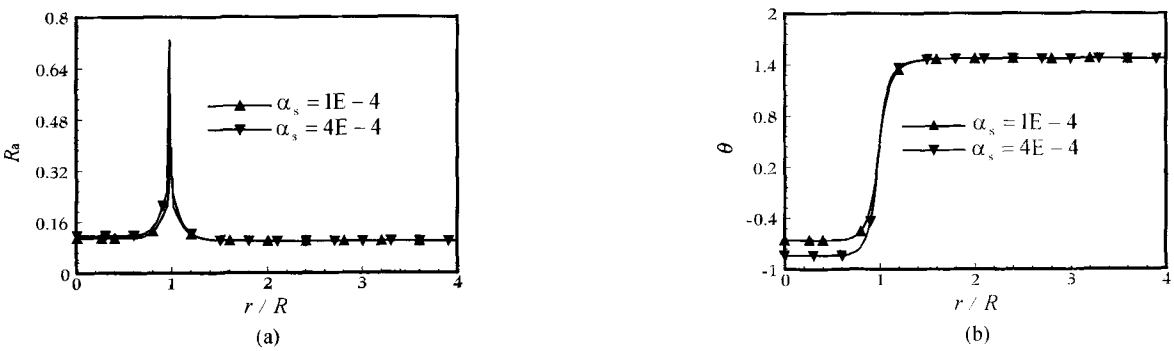

Fig. 4 Suspension-gas complex disturbance velocity ratio curves($\frac{\beta\theta}{\Delta U}$ = 0.1, U_∞ = 0, St = 10, n = 1)

(a) amplitude of velocity ratio; (b) disturbance phase difference

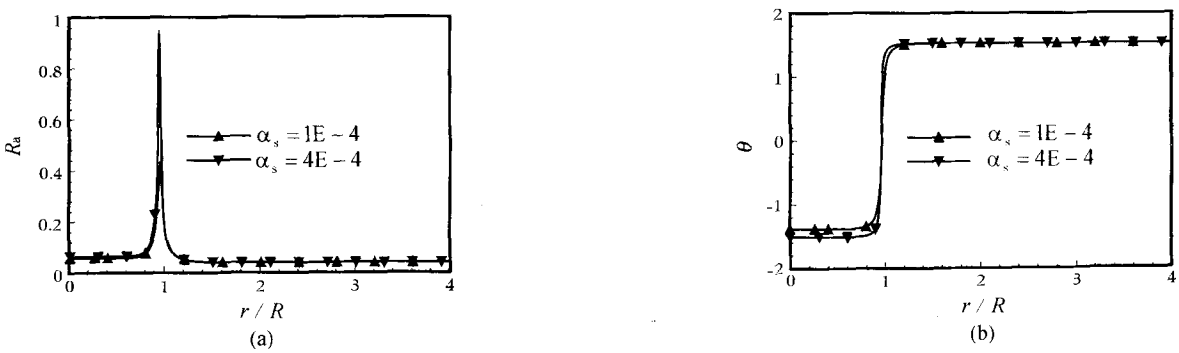

Fig. 5 Suspension-gas complex disturbance velocity ratio curves($\frac{\beta\theta}{\Delta U}$ = 0.25, U_∞ = 0, St = 10, n = 0)

(a) amplitude of velocity ratio; (b) disturbance phase difference

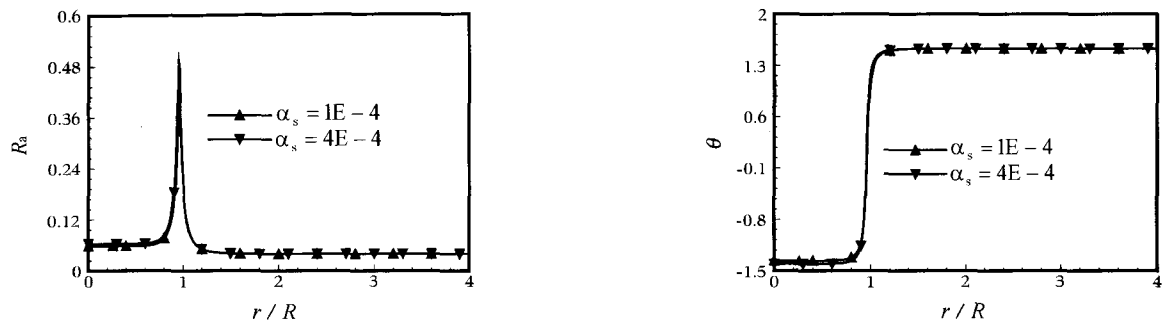

Fig.6 Suspension-gas complex disturbance velocity ratio curves($\frac{\beta\theta}{\Delta U}=0.25$, $U_\infty=0$, $St=10$, $n=1$)

(a) amplitude of velocity ratio; (b) disturbance phase difference

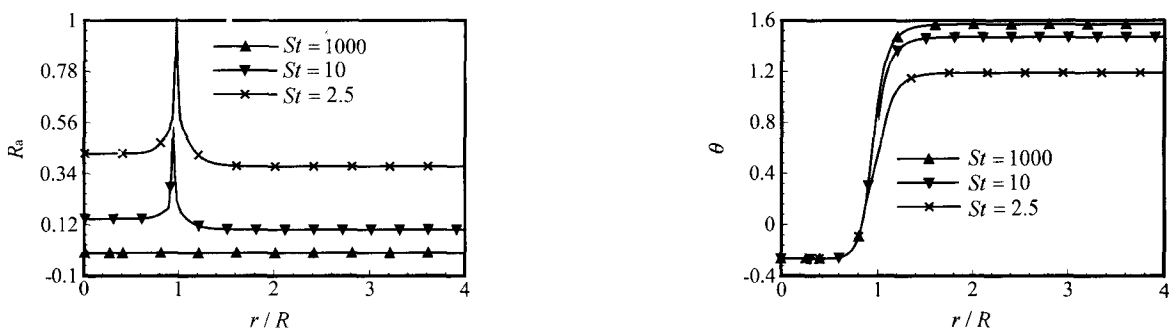

Fig.7 Suspension-gas complex disturbance velocity ratio curves($\frac{\beta\theta}{\Delta U}=0.1$, $U_\infty=0$, $\alpha_s=10^{-4}$, $n=0$)

(a) amplitude of velocity ratio; (b) disturbance phase difference

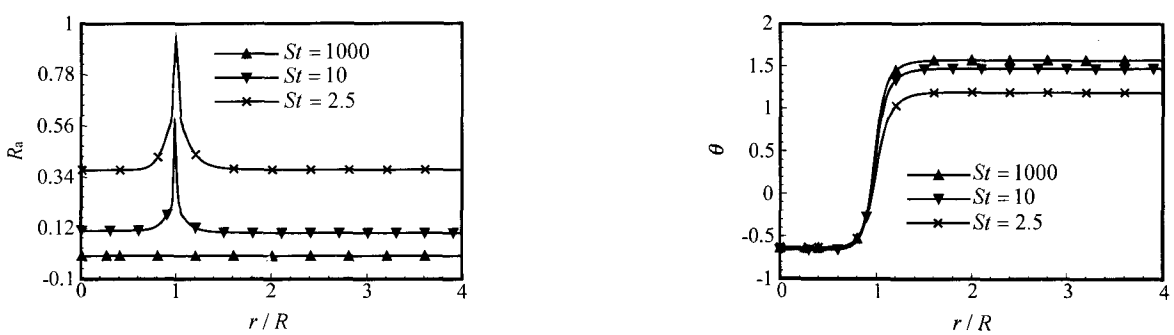

Fig.8 Suspension-gas complex disturbance velocity ratio curves($\frac{\beta\sigma}{\Delta U}=0.1$, $U_\infty=0$, $\alpha_s=10^{-4}$, $n=1$)

(a) amplitude of velocity ratio; (b) disturbance phase difference

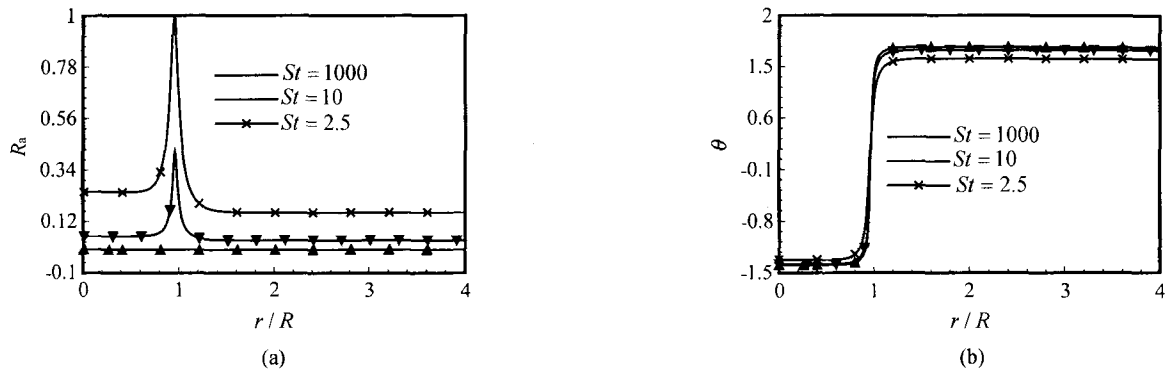

Fig.9 Suspension-gas complex disturbance velocity ratio curves($\frac{\beta\theta}{\Delta U} = 0.25$, $U_\infty = 0$, $\alpha_s = 10^{-4}$, $n = 0$)

(a) amplitude of velocity ratio; (b) disturbance phase difference

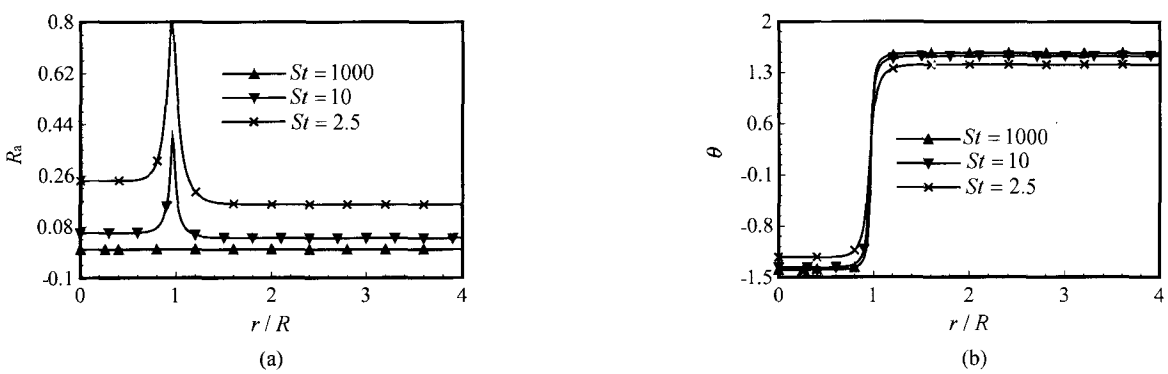

Fig.10 Suspension-gas complex disturbance velocity ratio curves($\frac{\beta\theta}{\Delta U} = 0.25$, $U_\infty = 0$, $\alpha_s = 10^{-4}$, $n = 1$)

(a) amplitude of velocity ratio; (b) disturbance phase difference

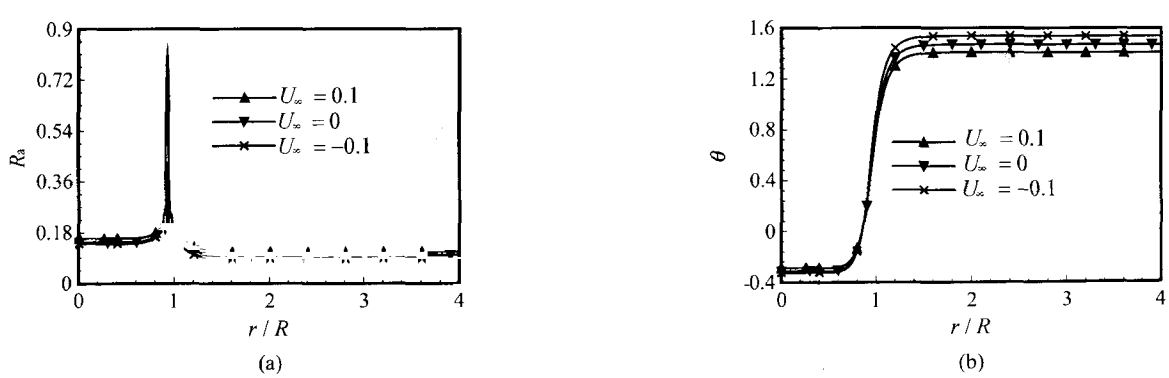

Fig.11 Suspension-gas complex disturbance velocity ratio curves($\frac{\beta\theta}{\Delta U} = 0.1$, $U_\infty = 0$, $\alpha_s = 10^{-4}$, $St = 10$, $n = 0$)

(a) amplitude of velocity ratio; (b) disturbance phase difference

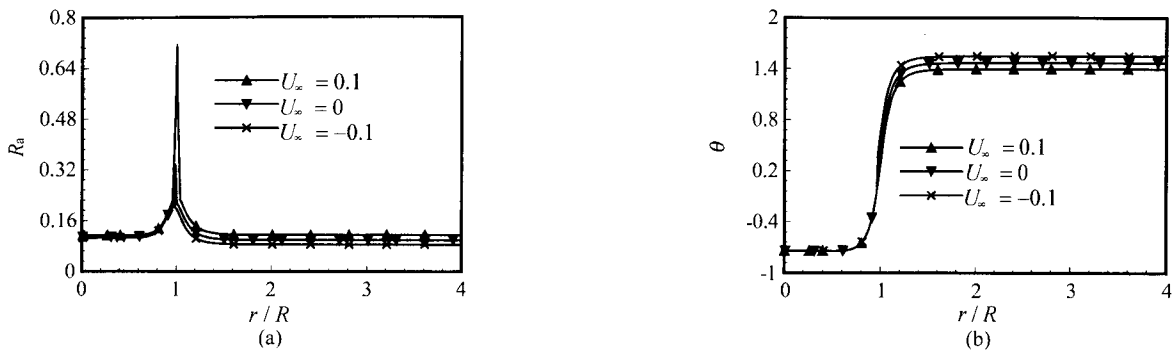

Fig.12 Suspension-gas complex disturbance velocity ratio curves($\frac{\beta\theta}{\Delta U} = 0.1, \alpha_s = 10^{-4}, St = 10, n = 1$)

(a) amplitude of velocity ratio; (b) disturbance phase difference

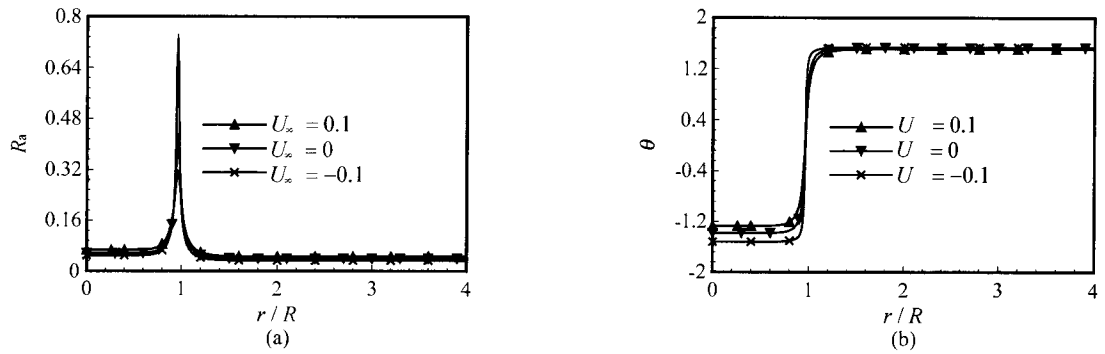

Fig.13 Suspension-gas complex disturbance velocity ratio curves($\frac{\beta\theta}{\Delta U} = 0.25, \alpha_s = 10^{-4}, St = 10, n = 0$)

(a) amplitude of velocity ratio; (b) disturbance phase difference

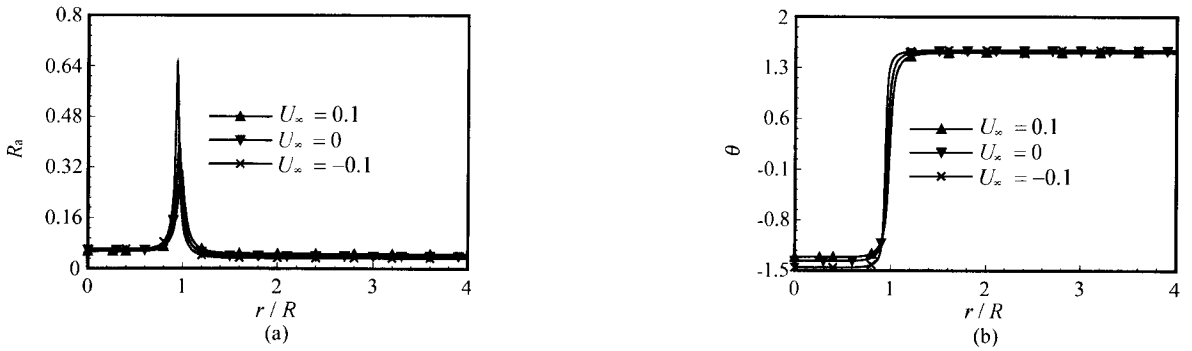

Fig.14 Suspension-gas complex disturbance velocity ratio curves($\frac{\beta\theta}{\Delta U} = 0.25, \alpha_s = 10^{-4}, St = 10, n = 1$)

(a) amplitude of velocity ratio; (b) disturbance phase difference

3. It can be found from Fig.3 to Fig.14 that whatever the nature of the field – flow and the properties of the suspensions are, the amplitude of the ratio reaches the maximum while the suspension – gas disturbance phase difference is zero at the critical point of the mean velocity profile. These demonstrate, according to Eq.(13), that the suspensions' ability to track the disturbed gas flow at the critical point is good compared with that at any other point.

4. It can be seen from Fig.3 to Fig.14 that whether the disturbance is symmetric or asymmetric larger frequency of disturbance leads to smaller amplitude of the ratio, smaller negative

suspension – gas disturbance phase difference but larger positive suspension – gas disturbance phase difference. According to Eq. (13), these reveal to us that the larger frequency of disturbance degrades the suspensions' ability to track the disturbed gas flow.

5. From Fig. 3 to Fig. 14, we can see that the amplitude of the ratio is a little bit larger, the negative suspension – gas disturbance phase difference is large and the positive one is small, in the case of symmetric disturbance compared with those in the case of asymmetric disturbance. Apparently, we can know based on Eq. (13) that the suspensions' ability to track the gas flow disturbed by symmetric disturbance is better than the suspensions' ability to track the gas flow disturbed by asymmetric disturbance.

6. With the increase of the suspension volume fraction, we can find from Fig. 3 to Fig. 6, the difference of amplitude of the ratio is slight, the negative suspension – gas disturbance phase difference increases but the positive one changes negligibly.

7. Fig. 7, Fig. 8, Fig. 9 and Fig. 10 show that the smaller equivalent Stokes number makes the amplitude of the ratio become larger, the negative suspension – gas disturbance phase difference becomes larger but the positive becomes smaller. These mean according to Eq. (13) that the smaller the equivalent Stokes number becomes, the better the suspensions' ability to track the disturbed gas flow becomes.

8. We can find from Fig. 11 to Fig. 14 that when the velocity of a jetting device varies from zero to any positive value, the amplitude of the ratio increases, the negative suspension – gas disturbance phase difference increases but the positive one decreases; but that when the velocity of the jetting device varies from zero to any negative value the case is contrary. Obviously, Eq. (13) tell us that positive velocity of jetting device can improve the suspensions' ability to track the disturbed gas flow but the effect of negative velocity is just the contrary.

The following conclusions on the disturbance properties of suspension near the injection area of a moving jet based on the discussions above can be obtained: suspension disturbance velocity is less than gas velocity; the suspension disturbance phase accords with the gas phase at the critical point, lags the gas phase between the axis and the critical point but leads the gas phase between the critical point and the far – field point; suspensions can track best the disturbed gas flow at the critical point; larger frequency of disturbance can degrade the suspensions' ability to track the disturbed gas flow; suspensions' ability to track the gas flow disturbed by symmetric disturbance is better than that to track the gas flow disturbed by asymmetric disturbance; the smaller the equivalent Stokes number becomes, the better the suspensions' ability to track the disturbed gas flow becomes; positive velocity of jetting device can improve suspensions' ability to track the disturbed gas flow but the negative velocity can degrade suspensions' ability to track the disturbed gas flow.

References

Alfons Michalke and Gunter Hermann, 1982. On the instability of a circular jet with external flow. *Journal of Fluid Mechanics*, **114**:343 – 359.

Chung, J. N., and Troutt, T. R., 1988, Simulation of particle dispersion in an axisymmetric jet. *Journal of Fluid Mechanics*, **186**:199 – 222.

Kong Kang, Qin Mengzhao, 1991. Hamilton algorithm of hamilton dynamic system. *Progress in Natural Science*, (**2**):102 – 112.

Lin Jianzhong, Shen Liping, Zhou Zexuan, 2000 . The effect of the coherent structures in the boundary layer flow on erosion. *Wear*, **241**:10 – 16.

Logmire, E. K., and Eaton, J. K., 1992. Structure of a particle – laden round jet. *Journal of Fluid Mechanics*, **236**:217 – 257.

Logmire, E. K., and Eaton, J. K., 1994. Active open – loop control of particle dispersion in round jets. *AIAA. Journal*, **32**:555 – 563.

Peterson, R. A., and Samet, M. M., 1988. On the preferred mode of jet instability. *Journal of Fluid Mechanics*, **77**:511 – 529.

Ramkumar N. Parthasarathy, 1995. Stability of particle-laden round jets to small disturbances. *FED-Gas-Particle Flow, ASME*, **228** :427 – 433.

Sykes, D., and Lyell, M. J., 1994. The effect of particle loading on the spatial stability of a circular jet. *Physics of Fluids*, **6**:1937 – 1939.

Yang, Y., Chung, J. N., Troutt, T. R., and Crowe, C. T., 1990. The influence of particles on the spatial stability of two-phase mixing layers. *Physics of Fluids A*, **2**: 1839 – 1845.

Zhou Zexuan, Lin Jianzhong, Wang Canxing et al., 1999. Disturbance property of suspensions lying on interface of moving two-phase jet. Proceedings' of 8th Asian Congress of Fluid Mechanics, Shenzhen, China, p.137 – 140.